# Case Study

# Aerodynamics of supercritical airfoils using Ansys Fluent Software

Developed and curated by the Ansys Academic Development Team

Ravindra Arjun Shirsath

education@ansys.com

© 2024 ANSYS, Inc.

## Ansys Software Used

This case study uses Ansys Fluent®, the fluid simulation software.

## Summary

Purely subsonic and purely supersonic flows are relatively easy to analyze and the aerodynamic characteristics of traditional airfoils under these conditions are observed to be as expected. However, when there occurs a mixed flow, the things start getting complicated. When an airfoil is operating at relatively higher Mach number, the regions of supersonic flow are observed around an airfoil due to local flow acceleration. These regions are often terminated by a strong shock that further causes flow separation thereby resulting in higher drag and lower lift. However, investigating an external flow past an airfoil at relatively higher speeds has always been fascinating as well as challenging. The strong need for computational solutions arises as conducting experiments to capture underlying flow physics, particularly at high speeds is not only time consuming but also costly. Further, the data acquisition and flow visualization techniques are complex as well as limited. Thus, Ansys Fluent Software, which is a popular commercial CFD software with vast capabilities including geometry preparation, meshing, solutions, and post processing makes it easy to predict accurate flow physics under various circumstances. Particularly, the accuracy and ability to predict formation of shocks, pressure and velocity variations and flow visualization at such high speeds are outstanding.

In the present case study, steady state simulations are performed over a NACA 0012 and SC(2)-0712 airfoils over a wide range of Mach numbers and are compared with. The investigations are further extended to understand the concepts of critical Mach number and drag divergence Mach number. The results include the variation of lift and drag coefficients with Mach number, pressure and Mach number distribution and flow visualization. The present study will serve as a starting point for mechanical, aeronautical, and aerospace engineering students to better understand the fundamental concepts associated with external aerodynamics along with the visualization of phenomenon of shock formation and drag divergence.

## Table of Contents

1. Introduction ..... 3
   1.1 Airfoil Designation ..... 3
2. Problem Statement ..... 4
3. Geometry and Mesh ..... 4
4. Solution Methodology ..... 4
5. Results and Discussion ..... 5
   5.1 Flow past NACA 0012 airfoil ..... 5
   5.2 Flow past SC(2)-0712 airfoil ..... 8
6. Further Steps ..... 11
7. References ..... 11


© 2024 ANSYS, Inc.

## 1. Introduction

The aerodynamic properties such as drag and lift coefficient experienced by an airfoil under the given operating conditions are greatly dependent on the shape of an airfoil itself. It is nearly impossible to have a single shape giving optimum performance under different operating conditions. Thus the airfoils meant for operating at relatively lower speeds are way different than the airfoils to be operated at high speeds. Generally, thick, cambered airfoils with rounded leading edges are preferred for low speed (subsonic) applications while thin, symmetrical airfoils with sharp leading edges are preferred for high speed (supersonic) applications. However, the transonic flow regime is the most critical as the lift and drag coefficients along with the pressure and velocity/Mach number distribution are distinctly different in transonic flow as compared to completely subsonic or supersonic flow. Transonic flow occurs when there is mixed sub- and supersonic local flow in the same flow field. Even if the incoming free stream Mach number is still subsonic, due to the acceleration of flow particularly around an airfoil mostly on the upper surface the flow may become supersonic. Usually, the supersonic region of the flow is terminated by a shock wave, allowing the flow to slow down to subsonic speeds. Shock waves are basically very thin regions across which the flow properties such as temperature, pressure, velocity, density etc. vary drastically.

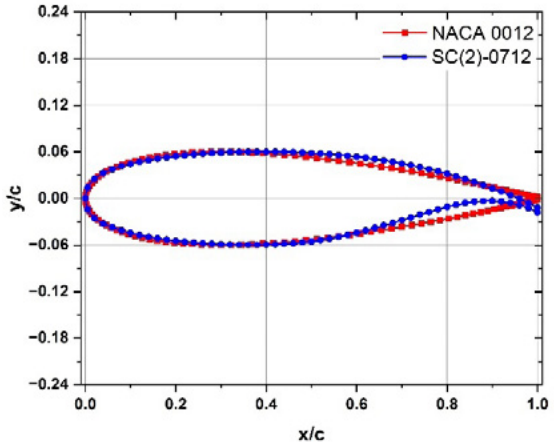


Figure 1. Comparison of NACA 0012 and SC(2)-0712 airfoil shapes.

The coordinated effort by National Aeronautics and Space Administration (NASA) during 1960's and 1970's provided major insights into the complicated flow physics under the transonic conditions. Resulting in the development of airfoils with a good transonic behavior while retaining acceptable low-speed characteristics that are popularly referred to as "Supercritical Airfoils". This distinctive airfoil shape as shown in Fig. 1, based on the concept of local supersonic flow with isentropic recompression, is characterized by a large leading edge radius, reduced curvature over the middle region of the upper surface and substantial aft camber.

### 1.1 Airfoil Designation

The airfoil designation is in the form SC(2)-0712, where SC(2) indicates Supercritical (phase 2). The next two digits designate the airfoil design lift coefficient in tenths (0.7), and the last two digits designate the airfoil maximum thickness in percent chord (12 percent).

***SC(2)-0712 Supercritical (phase 2) – 0.7 design lift coefficient, 12 percent thick.***

The aerodynamic characteristics of this airfoil are investigated computationally in the present work and the same are compared with those of NACA 0012 airfoil for the sake of better understanding.


© 2024 ANSYS, Inc.

## 2. Problem Statement

The aerodynamic characteristics of a NACA 0012 and SC(2)-0712 airfoils are investigated over a range of free stream Mach number at two different angles of attack, **α=0°** and **α=2°** focusing mainly on the Mach number and pressure variation. Increasing Mach number can cause shock stall and drag divergence, which can be understood by visualizing the pressure field, and investigating changes in the lift and drag coefficients.

## 3. Geometry and Mesh

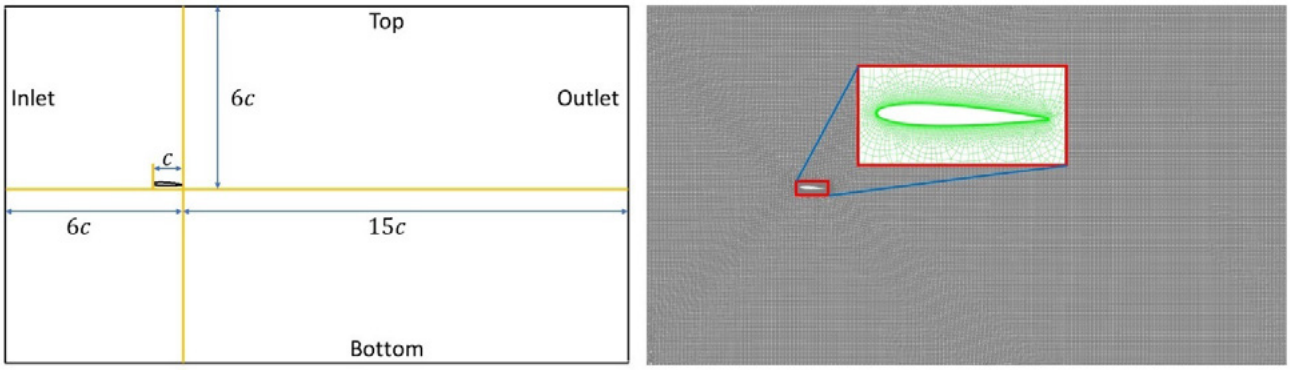


(a) Computational domain (b) Mesh.

Figure 2. Details of the geometry, mesh and computational domain.

The airfoil considered for present study has NACA 0012 (symmetric) profile. The computational domain used is shown in Fig. 2(a) that extends **6c** upstream as well as on top and bottom while **15c** downstream as it is mostly the downstream region which is highly influenced by the presence of the airfoil. The trailing edge of airfoil coincides with the origin. The mesh used for airfoil has **≈114000** nodes resulting in **≈113000** elements. Highly refined mesh is employed in the vicinity of the airfoil with layers of inflation and specified first layer height of $\mathbf{1.3x10^{-6}}$ to ensure that near wall phenomenon is captured correctly and the specific requirements of the selected turbulence model in terms of $\mathbf{y^+}$ are met. Though the mesh contains both quadrilateral and triangular elements, most of the domain predominantly consists of quadrilateral elements as seen from Fig. 2(b).

## 4. Solution Methodology

Using Ansys Fluent Software, the following methodology is used. Numerical solver is set up with pressure-based type, absolute velocity formulation and pressure-velocity coupling is dealt with SIMPLE algorithm. The working fluid is chosen to be an air as an ideal gas and dynamic viscosity modeled using Sutherland law. Least square cell-based method is employed for estimating the gradients while second order upwind scheme is used for discretizing the equations. The inlet is specified to be pressure far-field with the respective free stream Mach number, $\boldsymbol{M_\infty}$ with the turbulence properties specified through turbulent intensity of **1%** and turbulent viscosity ratio of **10**. Top and bottom boundaries are also imposed with the same condition while the outlet is set to be pressure outlet. Zero-gauge pressure is initialized throughout. The boundary at the airfoils is modeled to be solid wall. The selection of turbulence model is crucial, especially for the flows at higher Mach number. When using **k-ω** (SST) model, our computational results are seen to agree well with the experimental results, hence, **k-ω** (SST) is used throughout the analysis. The criterion for convergence is set to be $\mathbf{10^{-5}}$ and additionally the force coefficients on the airfoil are monitored individually ensuring that simulations are run for sufficient number of iterations.


© 2024 ANSYS, Inc.

## 5. Results and Discussion

This section first introduces important aspect concerning the variation of pressure and Mach number around an airfoil through contour plots for NACA 0012 airfoil for specific angles of attack of **α=0°** and **α=2°**. Corresponding aerodynamic coefficients for drag and lift are discussed subsequently along with their variation with Mach number over a wide range starting from low subsonic speed to high supersonic speed for both the angles of attack. The discussions are further extended for the super critical airfoil SC(2)-0712 under the above mentioned conditions for the systematic comparison of the overall aerodynamic performance of the two airfoils. The formation of shock wave and corresponding pressure distribution is also shown with the help of $C_p$-$x/c$ plots.

### 5.1 Flow past NACA 0012 airfoil

The Mach number and pressure contours for $M_\infty$=0.4 over NACA 0012 at **α=0°** as seen from Fig. 3(a) and (b) respectively, clearly indicates that though the flow is marginally accelerated around the point of maximum thickness resulting in the corresponding pressure variation as well, however it never reaches sonic condition anywhere. Noticeably being the symmetric airfoil at **α=0°** the variation of Mach number and pressure is exactly identical on the upper and lower surfaces hence resulting in no net pressure difference across and thus the lift produced is zero while a small amount of drag is observed.

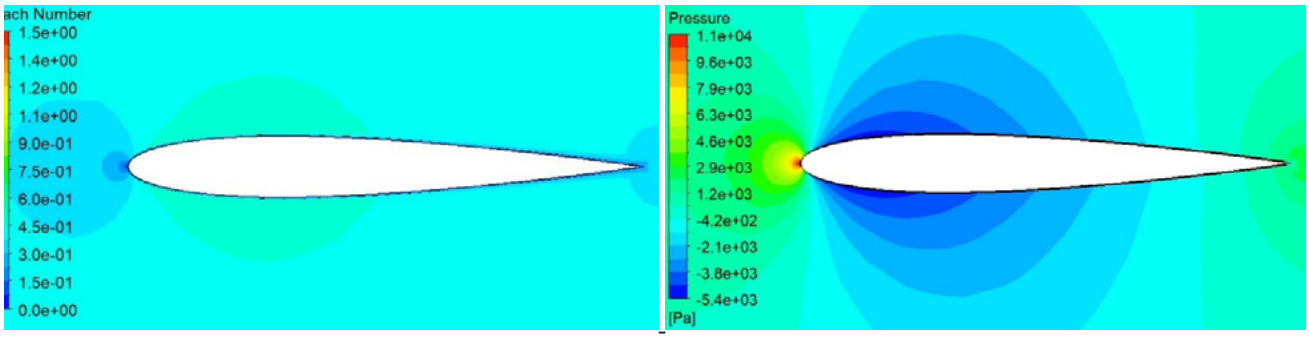


(a) Mach number contours. (b) Pressure contours.

Figure 3. Mach number and pressure variation over NACA 0012 airfoil at **α=0°** and $M_\infty$=0.4.

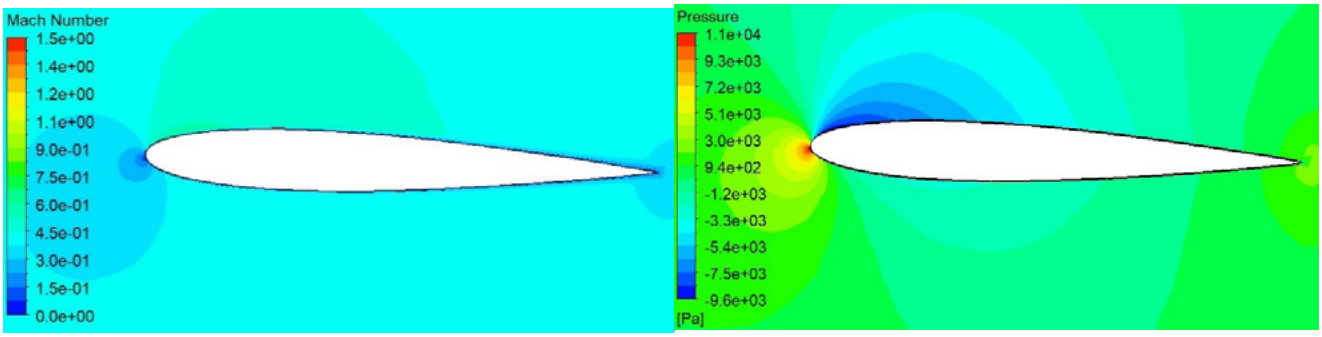


(a) Mach number contours. (b) Pressure contours.

Figure 4. Mach number and pressure variation over NACA 0012 airfoil at **α=2°** and $M_\infty$=0.4..

The effect of increasing the angle of attack to **α=2°** disturbs this symmetry as seen from Fig. 4(a) and (b) respectively and thus generates the pressure difference resulting in low pressure region on the upper surface and high pressure region on the lower surface thereby contributing to a positive lift. The Mach number however still remains subsonic throughout the domain and no traces of sonic or supersonic regions are observed yet.


© 2024 ANSYS, Inc.

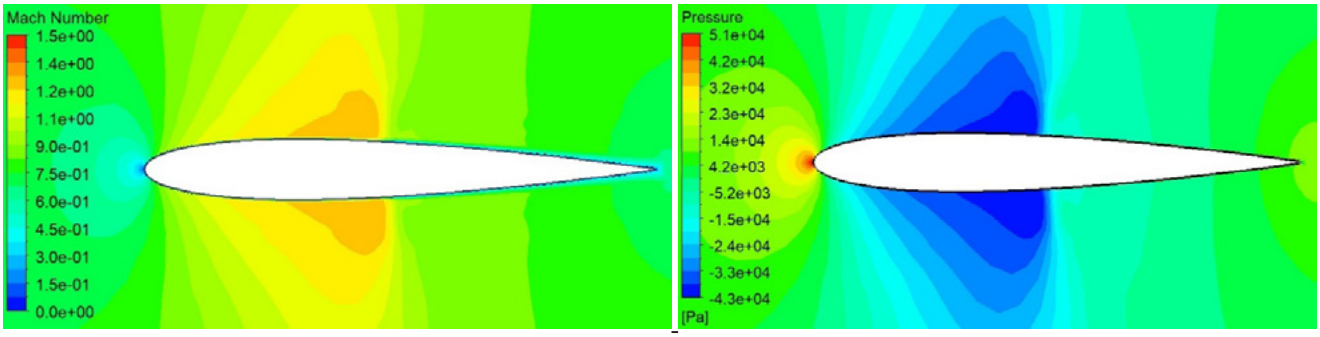


(a) Mach number contours. (b) Pressure contours.

Figure 5. Mach number and pressure variation over NACA 0012 airfoil at **α=0°** and ***M$_\infty$=0.8***.

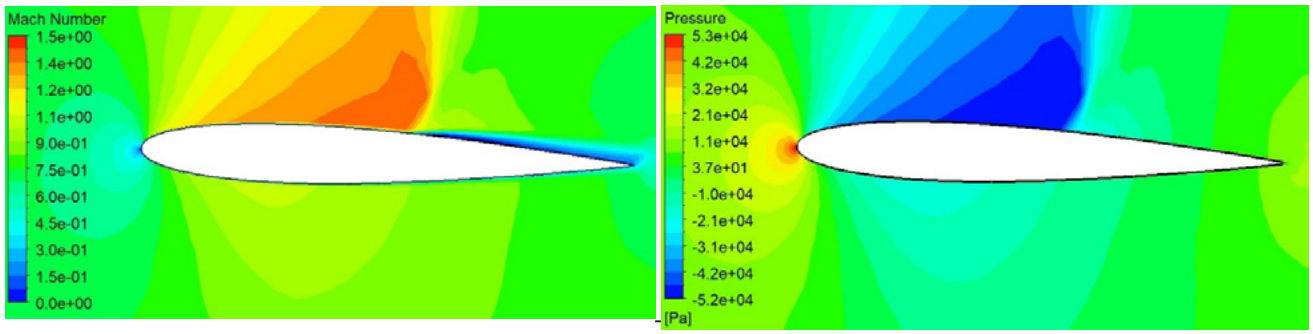


(a) Mach number contours. (b) Pressure contours.

Figure 6. Mach number and pressure variation over NACA 0012 airfoil at **α=2°** and ***M$_\infty$=0.8***.

Increasing the free stream Mach number from ***M$_\infty$=0.4*** to ***M$_\infty$=0.8*** leads to greater variation in Mach number and pressure contours, however at **α=0°** the symmetry is still retained between upper and lower surfaces as seen from Fig. 5(a) and (b) respectively. A small region of supersonic flow terminated by normal shock is also observed at around mid-chord location on either surface. The effect of this shock is clearly visible from the pressure contours causing drastic changes in pressure across the shock. Greater variation is observed particularly on the upper surface as the angle of attack is increased to **α=2°** as seen from Fig. 6(a) and (b) respectively with slightly aft movement of shock wave only on the upper surface while the changes on lower surface are still more gradual.

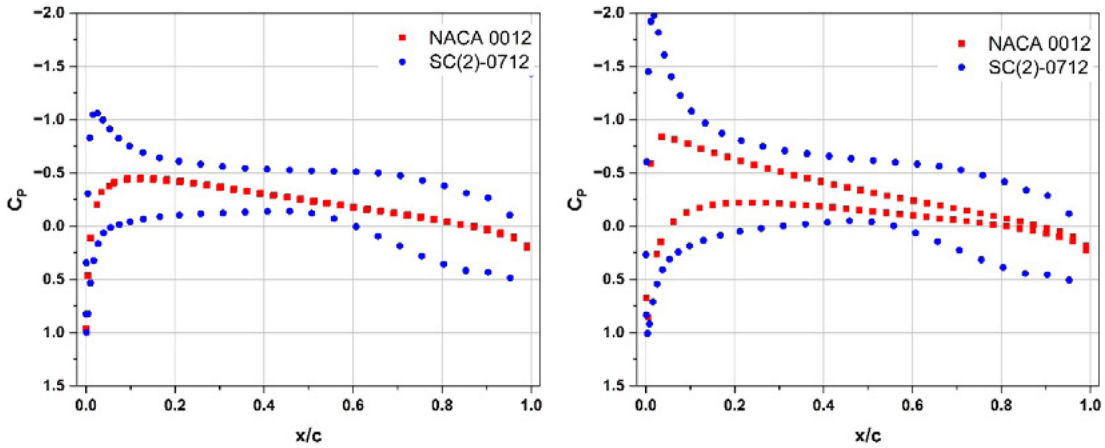


(a) ***C$_p$-x/c*** at **α=0°** (b) ***C$_p$-x/c*** at **α=2°**

Figure 7. Variation of pressure coefficient at ***M$_\infty$=0.4***.


© 2024 ANSYS, Inc.

The $C_p$-$x/c$ plot as seen from Fig. 7(a) for **α=0°** further clearly shows that for NACA 0012 the pressure distribution is identical between the two surfaces resulting in a single line while at **α=2°** the upper surface experiencing more negative $C_p$ compared to lower surface is evident from Fig. 7(b).

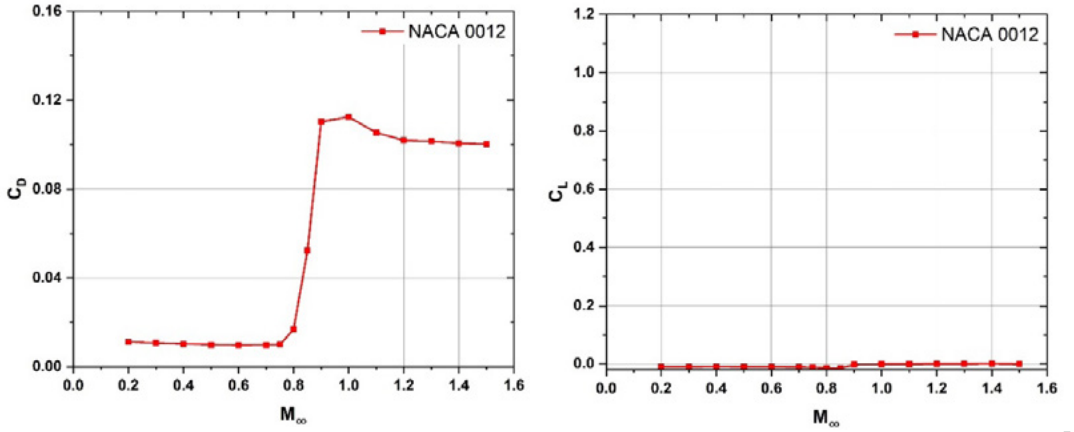


(a) Drag Coefficient, $C_p$. (b) Lift Coefficient, $C_L$.

Figure 8. Variation of drag and lift coefficients of NACA 0012 at **α=0°**.

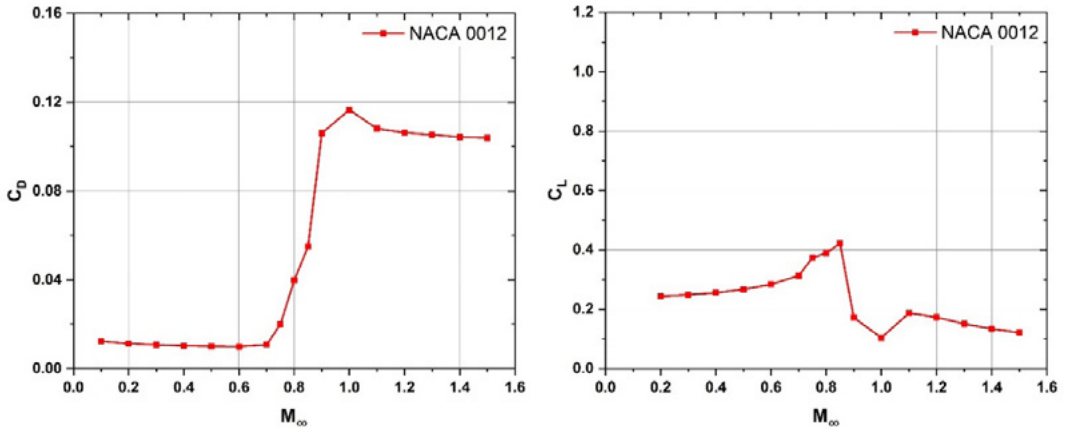


(a) Drag Coefficient, $C_D$. (b) Lift Coefficient, $C_L$.

Figure 9. Variation of drag and lift coefficients of NACA 0012 at **α=2°**.

The variation of aerodynamic coefficients with free stream Mach number is shown for **α=0°** in Fig. 8(a) and (b) respectively. As observed, the $C_D$ is relatively low for $M_\infty$<0.8 while is increases drastically beyond this Mach number due to the shock induced flow separation. The associated phenomenon is popularly known as "Shock Stall" and the corresponding free stream Mach number is referred to as Drag Divergence Mach Number. The $C_L$ on the other hand as seen from Fig. 8(b) is nearly zero and remains the same irrespective of the free stream Mach number, given that it is a symmetric airfoil. Thus under the said conditions an airfoil doesn't produce any lift while it experiences a considerable drag. Now for the airfoil to generate lift, an angle of attack is increased to **α=2°** and the corresponding variation of drag and lift coefficient is shown in Fig. 9(a) and (b) respectively. Under these operating conditions now the airfoil is observed to experience decent amount of lift, however the phenomenon of drag divergence still remains and the root cause for which is the relatively strong shock wave causing the drastic changes in flow properties and causing the flow separation. Thus it is important to have a design that can keep a check on these effects and hence super critical airfoils are introduced and discussed in the following section.


© 2024 ANSYS, Inc.

## 5.2 Flow past SC(2)-0712 airfoil

It is now known that due to acceleration of the flow, the Mach number at some point on the surface of an airfoil is higher than the free stream Mach number. Thus with increasing the free stream Mach number, there occurs a condition where the flow at least at a point reaches the sonic condition. This phenomenon is of a particular interest.

***Critical Mach Number ($M_{er}$)***– It is the free stream Mach number at which a sonic flow is observed for the first time at least at a point on the surface of an airfoil and is called the lower limit of transonic flow region or mixed flow pattern.

The name super critical comes from the fact that these are specially designed airfoils meant to operate satisfactorily even beyond the critical Mach number. As seen from Fig 10(a) and (b), the Mach number and pressure contours around SC(2)-0712 airfoil at **α=0°** and ***$M_\infty$=0.4*** indicates that given the relatively flat upper surface of these airfoils, the variation of Mach number and pressure is more gradual compared to the previous design. Also given that now the airfoil is not symmetric, a considerable difference in pressure is created between the upper and lower surfaces thereby contribution for a positive lift and that is further enhanced due to additional trailing edge camber on the lower side which is a trademark feature of a super critical airfoil.

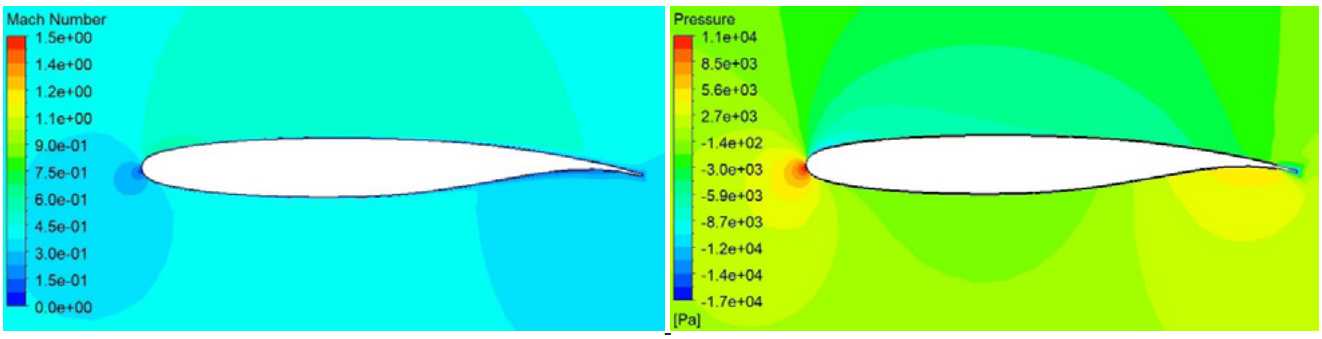


(a) Mach number contours. (b) Pressure contours.

Figure 10. Mach number and pressure variation over SC(2)-0712 airfoil at **α=0°** and ***$M_\infty$=0.4***.

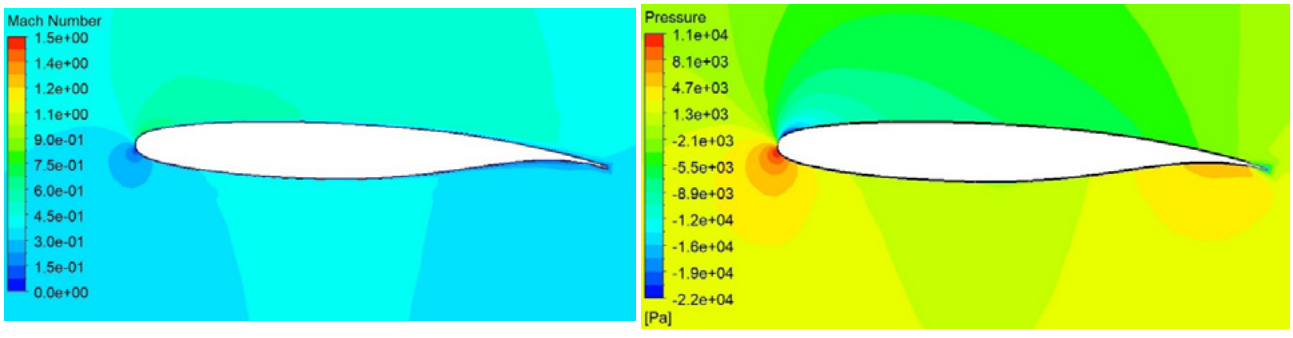


(a) Mach number contours. (b) Pressure contours.

Figure 11. Mach number and pressure variation over SC(2)-0712 airfoil at **α=2°** and ***$M_\infty$=0.4***

The variation in these properties is seen to further enhance with increasing an angle of attack to **α=2°** at the same free stream Mach number from Fig 11(a) and (b). Though accelerated, the flow still remains


© 2024 ANSYS, Inc.

subsonic throughout the domain under these free stream conditions and thus resulting in relatively low $C_D$ and considerably higher $C_L$. The corresponding $C_p$-$x/c$ plot as seen from Fig. 7(a) and (b) clearly indicate that this airfoil is capable of generating larger pressure difference compared to NACA 0012.

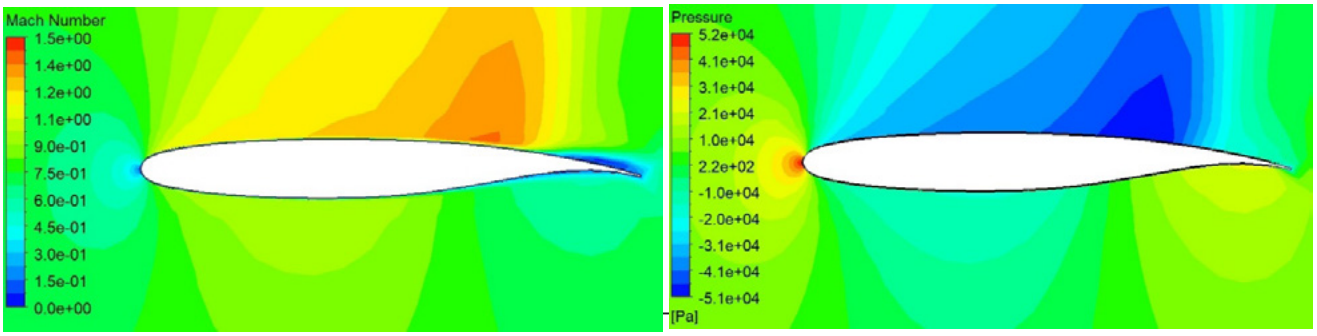


(a) Mach number contours. (b) Pressure contours.

Figure 12. Mach number and pressure variation over SC(2)-0712 airfoil at **α=0°** and $M_\infty$***=0.8***

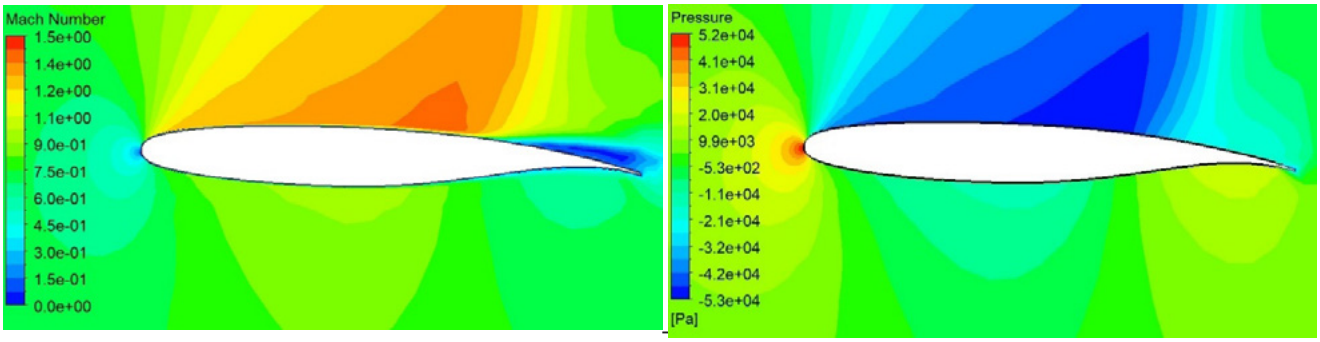


(a) Mach number contours. (b) Pressure contours.

Figure 13. Mach number and pressure variation over SC(2)-0712 airfoil at **α=2°** and $M_\infty$***=0.8***.

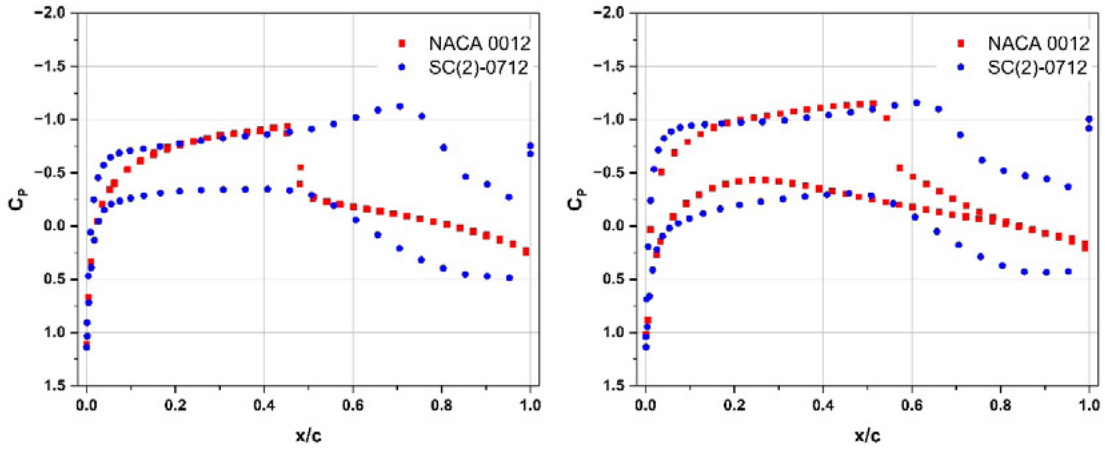


(a) $C_p$-$x/c$ at **α=0°** (b) $C_p$-$x/c$ at **α=2°**

Figure 14. Variation of pressure coefficient at $M_\infty$***=0.8***.

As the free stream Mach number is further increased to $M_\infty$***=0.8***, it is now seen from Fig. 12(a) that at **α=0°**, a considerable region of super sonic flow has developed on the upper surface however owing to relatively flat upper surface, the flow acceleration is mild. Additionally, the shock is much aft compared to the case of NACA 0012 causing relatively less change in pressure as seen from Fig. 12(b). Increasing the angle of attack further to **α=2°** causes these effects to enhance marginally as seen from Fig. 13(a)


© 2024 ANSYS, Inc.

and (b) respectively. The position of shock, variation of pressure across it and effect of aft camber is more evident from the $C_p$-$x/c$ plot as seen from Fig. 4(a) for **α=0°** and **α=2°** respectively.

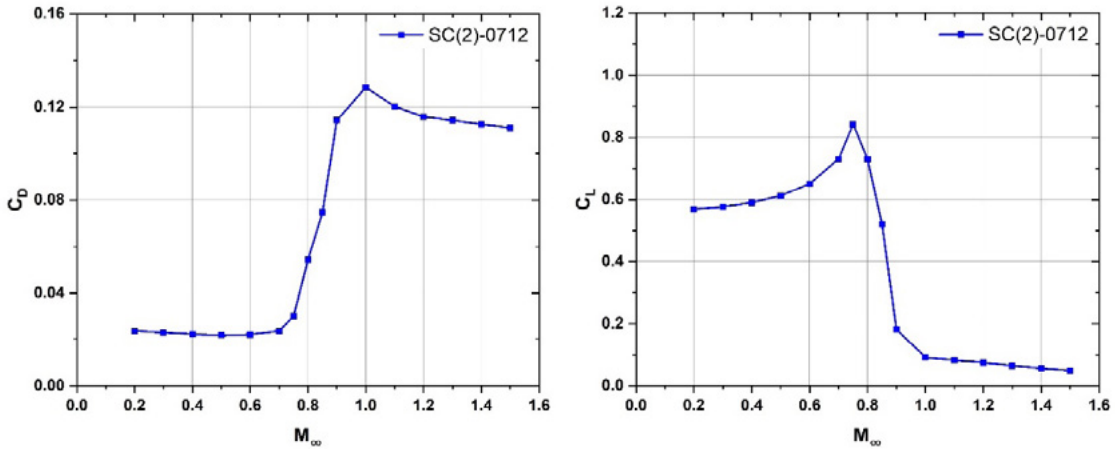


(a) Drag Coefficient, $C_p$. (b) Lift Coefficient, $C_L$.

Figure 15. Variation of drag and lift coefficients of SC(2)-0712 at **α=0°**.

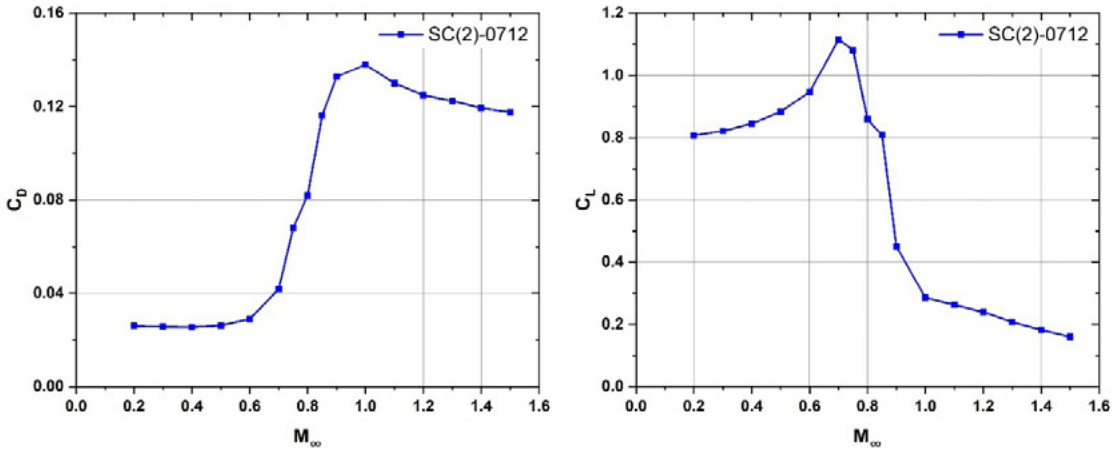


(a) Drag Coefficient, $C_D$. (b) Lift Coefficient, $C_L$.

Figure 16. Variation of drag and lift coefficients of SC(2)-0712 at **α=2°**.

The associated variation of $C_D$ and $C_L$ with for SC(2)-0712 airfoil at **α=0°** is shown in Fig. 15(a) and (b) respectively. Though the $C_D$ doesn't show much difference compared to that of NACA 0012, it is the $C_L$ that is considerably high compared to NACA 0012 where it was nearly zero. The $C_L$ is seen to further enhance with increasing angle of attack to **α=2°** without much effect on $C_D$ as seen from Fig. 16(a) and (b) respectively. Thus overall, the super critical airfoil SC(2)-0712 is observed to have much better aerodynamic performance as compared to NACA 0012 having same thickness over a wider range of Mach numbers.


© 2024 ANSYS, Inc.

## 6. Further Steps

In the present case study, the high-speed aerodynamic characteristics of NACA 0012 and SC(2)-0712 airfoil are investigated using Ansys Fluent Software. The investigation clearly shows that the highly complicated phenomenon of formation of shocks that results in mixed flow pattern can be investigated using advanced CFD software such as Ansys Fluent to predict the aerodynamic characteristics accurately. With the help of flow visualization through the contours of Mach number and pressure it is easy to demonstrate and understand the formation and movement of shock with varying Mach number.

These steady state investigations show preliminary analysis and the same can be extended to further investigate the performance of different airfoils, effect of thickness, camber and leading-edge nose radius of the airfoils. The effect of an angle of attack for a fixed Mach number can also be investigated. Additionally, transient simulations are expected to allow more investigation of how the shock wave and flow separation develop.

## 7. References

1. Charles D. Harris., NASA Supercritical Airfoils – A matrix of family related airfoils, NASA Technical paper 2969, 1990, Langley Research Center, Hampton, Virginia.

2. Richard T. Whitcomb, Review of Supercritical Airfoils, NASA Technical paper, 1974, Langley Research Center, Hampton, Virginia.

3. Ravindra A. Shirsath., Transonic aerodynamics of NACA 0012 airfoil using Ansys Fluent, Case Study, Ansys Software Pvt. Ltd. (https://www.ansys.com/academic/educators/education-resources/transonic-aerodynamics-of-naca-0012-airfoil-using-ansys-fluent).


© 2024 ANSYS, Inc.

**© 2024 ANSYS, Inc. All rights reserved.**

## Use and Reproduction

The content used in this resource may only be used or reproduced for teaching purposes; and any commercial use is strictly prohibited.

## Document Information

This case study is part of a set of teaching resources to help introduce students to topics related to fluids.

## Ansys Education Resources

To access more undergraduate education resources, including lecture presentations with notes, exercises with worked solutions, microprojects, real life examples and more, visit www.ansys.com/education-resources.

## Feedback

Here at Ansys, we rely on your feedback to ensure the educational content we create is up-to-date and fits your teaching needs.

Please click the link here out a short survey (~7 minutes) to help us continue to support academics around the world utilizing Ansys tools in the classroom.

**ANSYS, Inc.**
Southepointe
2600 Ansys Drive
Canonsburg, PA 15317
U.S.A.
724.746.3304
ansysinfo@ansys.com

If you've ever seen a rocket launch, flown on an airplane, driven a car, used a computer, touched a mobile device, crossed a bridge or put on wearable technology, chances are you've used a product where Ansys software played a critical role in its creation. Ansys is the global leader in engineering simulation. We help the world's most innovative companies deliver radically better products to their customers. By offering the best and broadest portfolio of engineering simulation software, we help them solve the most complex design challenges and engineer products limited only by imagination.

visit **www.ansys.com** for more information

Any and all ANSYS, Inc. brand, product, service and feature names, logos and slogans are registered trademarks or trademarks of ANSYS, Inc. or its subsidiaries in the United States or other countries. All other brand, product, service and feature names or trademarks are the property of their respective owners.

© 2024 ANSYS, Inc. All Rights Reserved.